Effect of diamagnetic dilution and non-stoichiometry on ESR spectra in manganites

2005 J. Phys.: Condens. Matter 17 1259

(http://iopscience.iop.org/0953-8984/17/7/018)

INSTITUTE OF PHYSICS PUBLISHING JOURNAL OF PHYSICS: CONDENSED MATTER

J. Phys.: Condens. Matter **17** (2005) 1259–1269 doi:10.1088/0953-8984/17/7/018

Effect of diamagnetic dilution and non-stoichiometry on ESR spectra in manganites

N Noginova[1], R Bah[1], D Bitok[1], V A Atsarkin[2], V V Demidov[2] and S V Gudenko[3]

[1] Norfolk State University, Norfolk, VA 23504, USA
[2] Institute of Radio Engineering and Electronics RAS, 125009 Moscow, Russia
[3] Russian Scientific Centre 'Kurchatov Institute', 123182 Moscow, Russia

Received 24 November 2004, in final form 4 January 2005
Published 4 February 2005
Online at stacks.iop.org/JPhysCM/17/1259

Abstract

ESR spectra are studied in a series of diamagnetically diluted manganites, single crystals of $LaGa_{1-x}Mn_xO_3$, in a broad range of the Mn ion concentration, $0 < x \leqslant 1$. With increase in Mn concentration, a complex multi-line spectrum, typical for low Mn concentrations, evolves to an exchange-narrowed several- or single-line spectrum at $x > 0.05$. The temperature behaviour of the ESR line-width in the range of 80–300 K is found to be very different in the materials with high ($x \geqslant 0.2$) and intermediate ($0.05 \leqslant x \leqslant 0.1$) concentration of Mn ions: a slight growth of the line-width is observed in the former case, while a steep line narrowing occurs at $x = 0.05$ and 0.1 with increase in temperature. Similar temperature dependence of the line-width is also observed for an additional ESR line arising in the non-stoichiometric oxygen-deficient $LaMnO_{3-\delta}$ manganite. We explain the experimental data by taking into account the effect of the thermo-activated Jahn–Teller reorientation process on spin dynamics in Mn clusters, and estimate its activation energy as 50–100 meV.

(Some figures in this article are in colour only in the electronic version)

1. Introduction

In the past few years, perovskite manganites (such as $La_{1-x}Sr_xMnO_3$, $La_{1-x}Ca_xMnO_3$, etc) have been extensively studied due to the discovery of the colossal magnetoresistance (CMR) effect and the rich complex diagram of phase transitions in these materials (see, for example, [1–3]). According to most theoretical models, magnetic and transport properties of these compounds are determined by interactions between Mn ions, including the double-exchange mechanism, associated with mobile electron exchange between Mn^{3+} and Mn^{4+} ions, and superexchange coupling between immobile spins.

In addition to the exchange interactions, there is a strong coupling of the spin system with the lattice, strongly affecting both magnetic and transport properties of manganites. The valence state of Mn^{3+} is $t^3_{2g\uparrow}e_{2g\uparrow}$ with one electron in the doubly degenerate $e_{2g\uparrow}$ state. Due to

the Jahn–Teller (JT) effect, oxygen octahedra distort along one of the crystal axes in the (001) plane, lifting the e_g degeneracy and lowering the energy of the occupied orbitals, $d_{3x^2-r^2}$ or $d_{3y^2-r^2}$. In CMR materials, the electron exchange between Mn^{3+} and non-JT Mn^{4+} ions results not only in spin and charge transfer, but also is accompanied by the displacement of the lattice distortion, the so-called JT polaron, which determines transport properties of these materials above the ferromagnetic transition.

In materials with a very high concentration of Mn^{3+} ions such as pure $LaMnO_3$, the static cooperative JT effect leads to Mn^{3+} ions having zig-zag-type ordering of occupied e_g orbitals in 001 planes. This system exhibits transition to the antiferromagnetic state ($T_N = 140$ K), with anti-parallel ferromagnetic-type ordering in the adjacent 001 planes. The orbital order exists up to $T_{JT} = 750$ K, where the cooperative phase transition occurs into a more symmetric state governed by the dynamic JT regime.

However, the diamagnetically diluted systems, such as $LaGa_{1-x}Mn_xO_3$, may demonstrate ferromagnetic and spin glass behaviour [4–6]. According to Goodenough [4, 5], in a magnetically dilute system the superexchange between two adjacent Mn^{3+} ions is expected to be ferromagnetic, due to a specific dynamic mechanism involving correlated Jahn–Teller vibrations of two Mn ions with the mutual orthogonal e orbitals. Note that the doping leads to the strong decrease of the temperature T_{JT} of the dynamic JT transition [5, 7], i.e., to significant decay of the JT orbital order.

To better understand the interplay of the exchange interactions and JT effect in manganite systems, we perform a systematic study of a series of magnetically diluted systems of $LaGa_{1-x}Mn_xO_3$ by the electron spin resonance method in a broad range of Mn concentrations (see also [8]). Such a study will provide specific information on type of spin–spin interactions and ordering in diluted manganites. As well, it has general interest as a study of the magnetic behaviour in diluted systems of magnetic dipoles in the conditions of strong coupling with the environment.

Besides, some data related to non-stoichiometric oxygen-deficient samples ($LaMnO_{3-\delta}$) will also be reported; as it will be seen, they are very similar to those obtained on the magnetically dilute materials and, perhaps, have the same origin.

2. Experimental details

Crystals of $LaGa_{1-x}Mn_xO_3$ with $0 \leqslant x \leqslant 0.5$ were grown by the Czochralski technique in a slightly oxidizing atmosphere. Materials with $0.5 \leqslant x \leqslant 1$ were fabricated by the floating zone technique. According to x-ray analysis, the lattice parameters depend on the composition in a way quite similar to the results reported in [5, 6]. Undoped $LaGaO_3$ has an orthorhombic O* structure with $a, b \sim c/\sqrt{2}$. $a = 5.489$, $b = 5.522$ and $c = 7.772$ Å (*Pnma* notation). $LaMnO_3$ has a distorted orthorhombic crystal lattice of O′ type ($c/\sqrt{2} < a, b$). With decrease of Mn concentration, the lattice changes from O' type ($c/\sqrt{2} < a, b$) at $x = 1$ to O* type ($a, b \sim c/\sqrt{2}$) at $x \leqslant 0.5$.

The so-called 'paper synthesis' (see, for example, [9]) was used to prepare the powders of $LaMnO_{3-\delta}$ with $\delta \sim 0.05$.

The ESR spectra were recorded using a standard Bruker EMX spectrometer, operating at 9.8 GHz (X-band).

3. Results

Regarding the appearance and temperature dependences of the ESR spectra, $LaGa_{1-x}Mn_xO_3$ materials can be divided into three large groups, namely, materials with low ($x = 0.005$ and 0.02), intermediate ($x = 0.05$, 0.01) and high ($x \geqslant 0.2$) concentration of Mn ions.

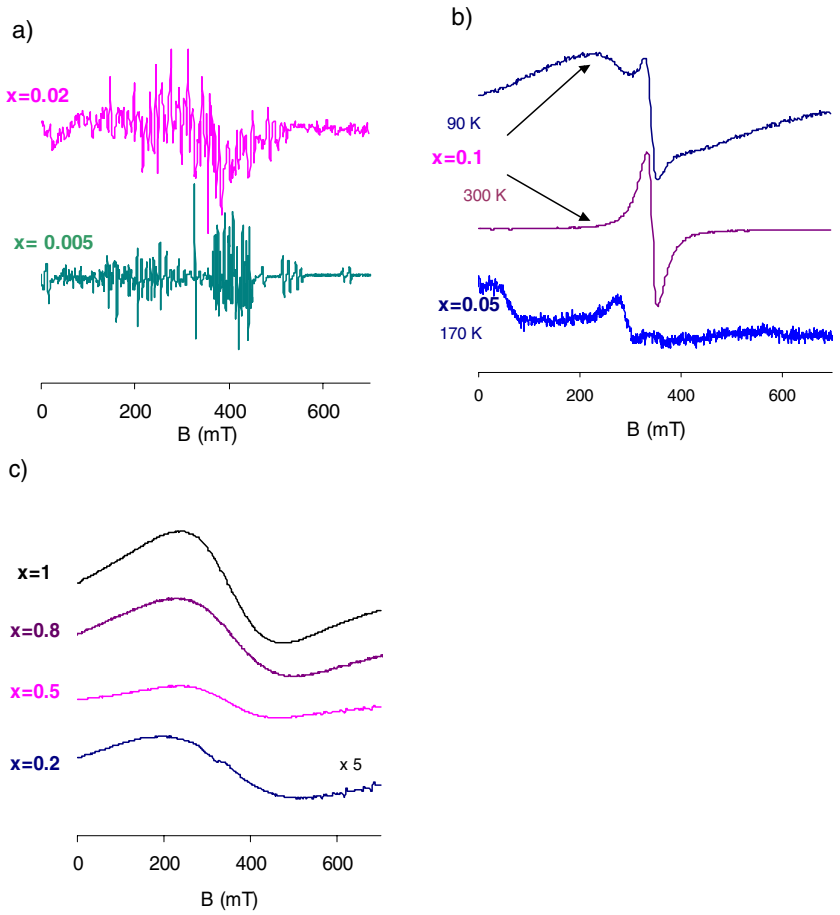

Figure 1. Typical ESR spectra in $LaGa_{1-x}Mn_xO_3$ at low concentration, $T = 293$ K (a), intermediate concentration (b), and relatively high concentration (c) of Mn ions, $T = 293$ K.

Samples with low Mn concentration, $x = 0.005$ and 0.02, demonstrate a multi-line ESR spectrum which consists of a huge number of narrow lines (figure 1(a)). One or several broader lines were observed in materials with intermediate Mn concentration (figure 1(b)). Materials with the concentration $x \geqslant 0.2$ demonstrate a single very broad line (figure 1(c)). Besides a different appearance of the spectra in the samples with intermediate and high x, the temperature behaviour is completely different as discussed below.

The estimation of the number of Mn ions contributing to the spectrum is around the nominal concentration for the materials $x \geqslant 0.2$, 10–20% of the nominal concentration for $x > 0.1$, and about 1% in the materials with $x \leqslant 0.05$.

Materials with $x \geqslant 0.5$ demonstrate a dependence of the position and width of the ESR line on the orientation of the crystal; see figure 2. This dependence becomes weaker with decrease in Mn concentration. The amplitude of the variation of the width with orientation ranges from 40% of the width at the concentration $x = 1$ (see also [10]) to ~10% at $x = 0.8$, and about ~1% at $x = 0.5$.

Thus, the angular dependence of the line-width in the dilute materials is rather weak, so the orientation is not specified throughout this paper unless otherwise indicated.

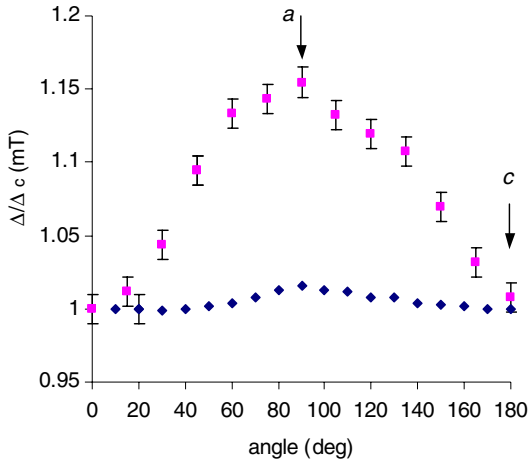

Figure 2. The width in dependence on the orientation (at the rotation around axis $b \perp \mathbf{B}$) in $LaGa_{0.5}Mn_{0.5}O_3$ (diamonds) and $LaGa_{0.2}Mn_{0.8}O_3$ (squares).

The temperature dependence of the resonance field B_0 (i.e. apparent g-factor) was also observed. The shifts of B_0 are larger at higher Mn concentration. They increase upon cooling according to the model accounting for the combined effect of the sample magnetization and zero-field splitting [10]. Besides, the effect of the 'anti-Larmor' term, especially pronounced for very broad EPR lines, causes an additional apparent shift of B_0 toward lower values. The data on the susceptibility, χ_{ESR}, estimated through double integration of the spectra or analysis of the fitting parameters, point to the ferromagnetic type of exchange interaction in the materials with $0.05 < x < 1$. At high enough temperatures χ_{ESR} can be approximately fitted with the Curie–Weiss law as

$$\chi_{ESR} = \frac{C}{T - \theta}, \tag{1}$$

where C is the Curie constant, T is the temperature, and θ is the Curie–Weiss temperature.

Materials with $x = 0.8$ and 0.5 demonstrate ferromagnetic transition at about 110 and 80 K correspondingly. Below the transition temperature, distortion and shift of the resonance line is observed, typical of the ferromagnetic resonance (FMR) behaviour. No transition was reached at $x = 0.2$ or less; however, the temperature dependence of χ_{ESR} points to the ferromagnetic character of the ordering ($\theta \cong 80$ K at $x = 0.2$ and $\theta \cong 64$ K at $x = 0.1$). A significant drop in the signal intensity was observed at $x = 1$ (pure $LaMnO_3$ crystal) in the range of 150 K, indicating antiferromagnetic transition, as can be expected in this material [1–3].

Below the transition temperature, materials with $x = 0.8$ demonstrated irreversibility and difference between zero-field cooling and field cooling (see figure 3), pointing to the existence of ferromagnetic hysteresis. The change of the orientation of the sample at low temperature led to similar effects: the ESR signal recorded during a first run after orientation change differs from the signals recorded in subsequent runs.

The ferromagnetic type of ordering observed in our diluted materials with $x \geqslant 0.2$, the transition temperatures and the irreversibility effects correspond well to literature data on similar materials [5, 6].

Let us now discuss the ESR spectra in the materials with the intermediate and high concentration of Mn in more details. In the materials with intermediate concentration, $x = 0.05$ and 0.1, the ESR spectrum consists of one, two or sometimes several lines (see figure 1(b)),

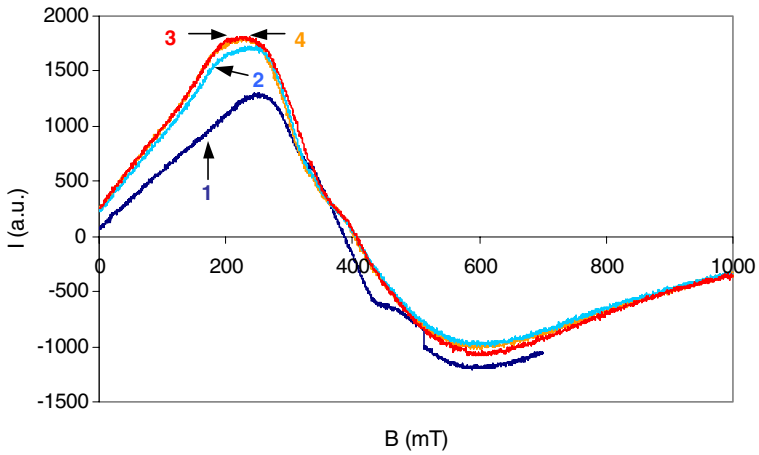

Figure 3. ESR signal in $LaGa_{0.2}Mn_{0.8}O_3$ at 103 K after zero-field cooling, first (trace 1) and second (trace 2) run, and after cooling in a field of 0.7 T, first and second runs (traces 3 and 4 overlap).

depending on the temperature and a particular sample. Samples cut from different sites of the crystal demonstrate slightly different spectra. The annealing of samples in oxygen leads to a slight broadening of the central line. However, all samples with $x = 0.05$ and 0.1 exhibit similar character of changes in the ESR spectrum with variation of temperature.

As an example, at room temperature, the spectrum in $LaGa_{0.9}Mn_{0.1}O_3$ can be described with a single line of approximately Lorenzian shape (figure 1(b), trace corresponding to 300 K). At lower temperatures, the second broader line appears (see figure 1(b), 90 K), rapidly growing and broadening with decrease in temperature. The temperature dependence of the width of this broad line is shown in figure 4(a). As one can see, with increase in temperature, substantial narrowing of the spectral width occurs, pointing to the presence of a thermo-activated process.

A single broad line is observed in materials with $x \geqslant 0.2$. In contrast to the previous case, in a broad temperature range, the width of the ESR signal demonstrates a slight growth with increase in temperature; see figure 4(b). Only at low temperatures, in a narrow temperature range, is some broadening of the spectra observed, pointing to approaching the ferromagnetic (at $x = 0.5$, 0.8) or antiferromagnetic (at $x = 1$) transition temperatures (the transition temperatures are indicated in figure 4(b) with arrows).

It is instructive to compare the data reported above with those related to the oxygen-deficient $LaMnO_{3-\delta}$ material where a number of Mn^{3+} ions may be transformed into the Mn^{2+} ones. The measurements are performed in the temperature range of 100–540 K. Typical ESR spectra at various temperatures are shown in figure 5. One can see that, apart from the broad line which is characteristic of the concentrated manganite (compare with the upper trace in figure 1(c)), an additional ('narrow') line is clearly seen. The double-integrated area of this additional line amounts to 1%–3% of the main ('broad') line intensity, whereas its line-width decreases steeply as temperature increases (figure 6). Obviously, the latter finding is quite similar to the temperature behaviour of the ESR line-width in magnetically dilute samples with $x = 0.05$–0.1; see figure 4(a). A possible explanation will be discussed in the next section.

4. Discussion

According to the estimations in the literature [10–12], the main contributions to the spin Hamiltonian of the manganite spin system are the Zeeman interaction with the static magnetic

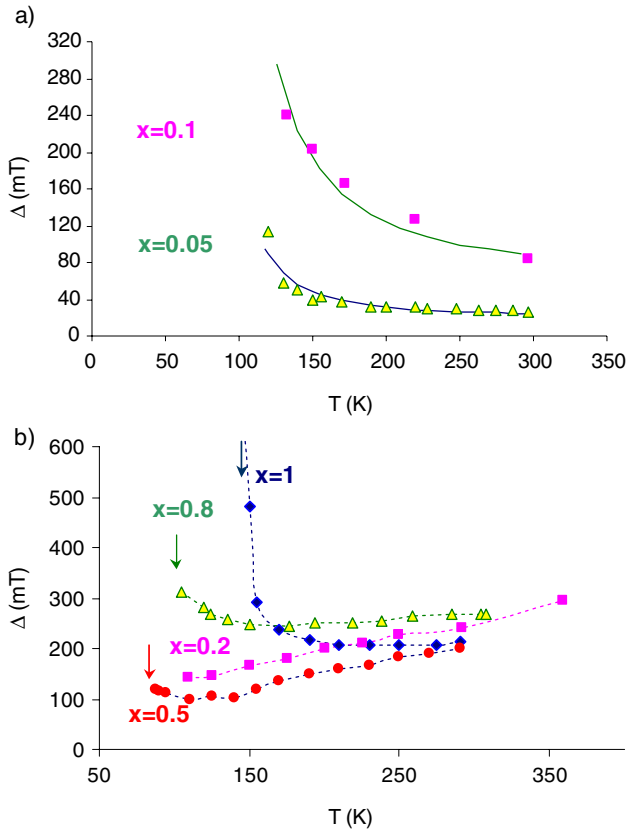

Figure 4. (a) The width of the broad ESR line in $LaGa_{1-x}Mn_xO_3$ with $x = 0.05$ (triangles) and $x = 0.1$ (squares). Solid curves are fitted with equation (5). (b) The width of the ESR line in the samples with high concentration of Mn ions of $x = 0.2$ (squares), $x = 0.5$ (circles), 0.8 (triangles) and 1 (diamonds). The arrows indicate the transition temperatures. Dashed curves are guides for the eye.

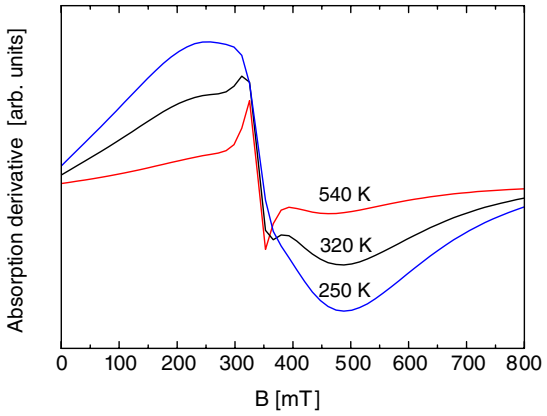

Figure 5. ESR spectra in $LaMnO_{3-\delta}$ at various temperatures (indicated by the traces).

field H; isotropic exchange coupling between neighbouring Mn spins, $\mathbf{S}_i$ and $\mathbf{S}_j$; crystal field (CF); and antisymmetric Dzyaloshinsky–Moriya (DM) interaction.

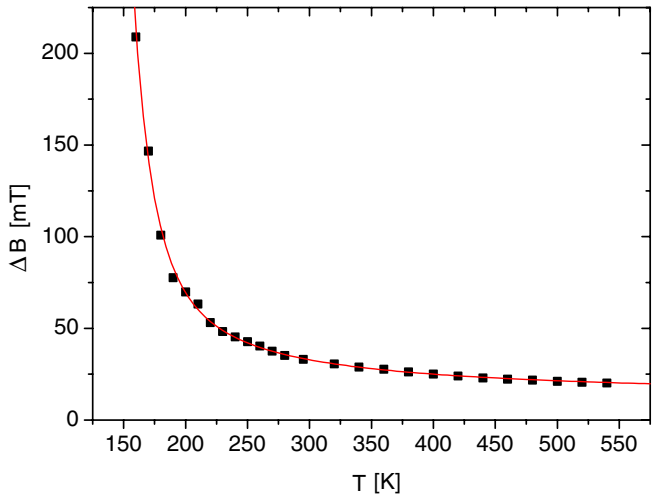

Figure 6. The width of the 'narrow' ESR component in $LaMnO_{3-\delta}$ plotted against temperature. The solid curve is the sum of two Arrhenius terms, as described in the text.

Taking into account these contributions, the spin Hamiltonian reads

$$\mathcal{H} = -\mu_B \sum_i \mathbf{H} g \mathbf{S}_i + J \sum_{(i<j)} \mathbf{S}_i \mathbf{S}_j + \sum_i (-D S_{z(i)}^2 + E(S_{x(i)}^2 - S_{y(i)}^2)) + \sum_{(i<j)} \mathbf{D}_{DM}[\mathbf{S}_i \times \mathbf{S}_j] + \mathcal{H}_1 \tag{2}$$

where μ_B is the Bohr magneton, g is the g-factor, J is the isotropic exchange integral, D and E are the crystal field constants, $\mathbf{D}_{DM}$ is the Dzyaloshinsky–Moriya matrix, and $\mathcal{H}_1$ includes the other terms such as dipole–dipole and hyperfine interactions. The subscripts $x(i)$, $y(i)$, and $z(i)$ used in the CF term denote the local symmetry axes in a given site (i) in the lattice; note that there are four magnetically non-equivalent sites in the perovskite unit cell. The CF and DM parameters are considered in equation (2) as static ones, that is, the dynamic JT effect is not explicitly included. We suppose that in the dynamic JT regime these parameters are changed for their averaged values, such as $\langle D \rangle$, $\langle E \rangle$, etc.

According to [10–12], in the $LaMnO_3$ material typical values of these contributions are in the order of 10 K for the isotropic exchange integral, and $\sim$1 K for the crystal field and Dzyaloshinsky–Moriya parameters.

In diluted materials with different concentrations of Mn ions, a major role is played by the different terms; the magnitude and dynamic of these interactions can also be different. Crystals with low concentrations of Mn correspond to the case of single isolated ions; in this simple case the spectra are determined primarily by the Zeeman, crystal field and hyperfine interactions. As known from the data of optical spectroscopy [13], at low doping concentration in lanthanum gallates, in addition to the majority of the Mn^{3+} ($S = 2$) state, some Mn ions can be present in different valence states such as Mn^{2+} ($S = 5/2$), Mn^{4+} ($S = 3/2$) and Mn^{5+} ($S = 1$). The spectrum for each of the valence states exhibits fine and hyperfine structure (the nuclear spin of ^{55}Mn, $I = 5/2$); besides, the total number of lines increases fourfold due to the four different non-equivalent positions of Mn at an arbitrary crystal orientation. These factors would explain hundreds of the narrow lines observed in the low doped samples. Note that the Mn^{3+} ions are non-Kramers ones ($S = 2$), and hence their energy spectrum includes zero-field splitting which might be beyond the X band used in our experiments.

Broad lines observed in materials with higher concentration of Mn are results of collective behaviour of Mn^{3+} ions. This is confirmed by the estimation of the number of Mn ions contributing to the spectra: as mentioned earlier, it nearly corresponds to the nominal Mn concentration in the materials $x \geqslant 0.2$. According to our experiments, all materials with $x \geqslant 0.2$ demonstrate behaviour similar to that observed in pure $LaMnO_3$ ($x = 1$) discussed in detail in [11, 12], such as a weak temperature dependence at high temperatures as well as a critical broadening in the vicinity of the magnetic transition.

In the conditions of strong exchange, the width of the line, Δ, is determined by

$$\Delta = \frac{M_2^0}{J} f(T), \tag{3}$$

where $M_2^0 \ll J$ is the second spectral moment arising from the anisotropic terms of the Hamiltonian, equation (2). The first ratio in equation (3) is conventional (see, for instance, [10]), whereas $f(T)$ is the function introduced by Huber [11]:

$$f(T) \propto (\chi T)^{-1}, \tag{4}$$

where χ is the static magnetic susceptibility. This function describes the moderate broadening of the ESR line well above the transition temperature.

Due to the effect of the strong exchange narrowing (see equation (3)) in $LaMnO_3$ one observes a single Lorentzian ESR line with the width Δ of about 0.2 T instead of a complicated spectrum with spectral width more than 1 T to be determined only by the crystal field and DM interactions. A similar picture is also observed in our samples with high ($x \geqslant 0.2$) concentration of Mn.

With increase in degree of dilution, the behaviour of spectral width is affected by the competition of two factors. First, the decrease in x leads to the decrease of the exchange integral, J, which would lead to spectral broadening. On the other hand, the anisotropic part of the Hamiltonian decreases due to the transition from the static to dynamic JT effect and consequent changes in crystal lattice, leading to the decrease of the second moment and narrowing of the spectra. The second factor explains the decrease in anisotropy of the spectral width with decrease in Mn concentration (see figure 2). Note that a stepwise reduction of the ESR line-width at T_{JT} was observed in concentrated manganites [12, 14].

Critical change in the behaviour occurs when the Mn concentration drops from $x = 0.2$ to 0.1. The strong line narrowing observed in the $x = 0.05$ and 0.1 samples with increase in temperature points to the significant effect of thermally activated motion that averages the anisotropic part of the spin Hamiltonian.

Let us assume that the halfwidth Δ of the ESR line under consideration is described by the formula

$$\gamma_e \Delta = \omega_L^2 \tau_e + \gamma_e \Delta_0 \tag{5}$$

where the first term is well known for the line narrowing induced by internal fast motion, ω_L is the magnitude of the fluctuating local field leading to the transversal spin relaxation [15], and Δ_0 is the temperature independent contribution arising from those parts of the spin Hamiltonian which cannot be averaged by the motion, γ_e is the gyromagnetic ratio, and τ_e is the correlation time, decreasing with temperature as

$$\tau_e = \tau_e^0 \exp\left(\frac{E_a}{kT}\right). \tag{6}$$

As one can see from figure 4(a), the experimental data can be fitted by equation (5) with parameters $E_a/k = 400$ K; $\Delta_0 = 50$ mT, $\tau_e^0 \omega_L^2 = 1 \times 10^5$ c^{-1} in the material with $x = 0.1$, and $E_a/k = 550$ K, $\Delta_0 = 20$ mT, and $\tau_e^0 \omega_L^2 = 14 \times 10^5$ c^{-1} at $x = 0.05$. A significant

number of fitting parameters as well as a relatively moderate range of the line-width variation with temperature allow us to speak only qualitatively; nevertheless, these results confirm that thermally activated motion with the activation energy of about 400–600 K does exist in our material and strongly affect the magnetic behaviour of the Mn^{3+} ions in the case of intermediate concentration.

The data on nuclear spin relaxation [16] also indicate the presence of such motion in low doped Mn:$LaGaO_3$ materials, with the correlation time following the Arrhenius law with the activation energy of 450–550 K.

We believe that this energy corresponds to the energy barrier between adjacent JT configurations in magnetically dilute manganite materials, so the internal motion under consideration is the thermally activated re-orientations of the JT orbitals and corresponding lattice distortions. The activation energy of 400–600 K is of an order of magnitude less than the JT energy of Mn^{3+} in the manganites [1–3]. However, one can expect that the barrier for JT reorientations is much lower than the peak JT energy; see for example [17].

A similar explanation may be appropriate for the oxygen-deficient sample, $LaMnO_{3-\delta}$. The appearance of two distinct ESR lines (figure 5) can be considered as evidence for the formation of large enough clusters which contain, along with the Mn^{3+} ions, the Mn^{2+} ones, as well as the oxygen vacancies. These clusters are, in some sense, analogous to those formed by Mn^{3+} ions at intermediate Mn concentration ($x = 0.05$–0.1) in the $LaGa_{1-x}Mn_xO_3$ lattice. Inside the clusters, the orbital order weakens and allows for the thermally activated re-orientations of the JT configurations. The solid curve in figure 6 fits the observed temperature dependence of the 'narrow' line-width in $LaMnO_{3-\delta}$ by a sum of two Arrhenius terms similar to equations (5), (6), with the activation energies of 300 and 1660 K. These values are of the same order of magnitude as the energy barriers found for $x = 0.05$ and 0.1, and it seems to be natural to ascribe them to the same physical process.

Another possible source of thermoactivated motion can be related to hopping of a small polaron associated with a hole localized on the Mn^{4+} ion. (The presence of some Mn^{4+} ions is confirmed in the samples with low concentration of Mn, as was mentioned earlier.) However, the values of the activation energy for the polaron hopping as determined from the conductivity measurements on the same $LaGa_{1-x}Mn_xO_3$ crystals [18] are within the range of 0.45–0.65 eV, an order of magnitude larger than the activation energy estimated in our experiments, $E_a \sim 50$ meV. In addition, according to the theory, thermally activated polaron hopping would result not in narrowing but broadening of the ESR line [19], in contrast to what is experimentally observed.

In our opinion, the experimental results allow us to consider the following scenario for spin interactions and ESR in diluted manganite systems. In materials with low concentration, the ESR spectra are determined by isolated ions. The increase in Mn concentration leads to the formation of Mn pairs and clusters in the materials with intermediate concentration, and to a dense exchange-coupled array of Mn ions at high concentration. Based on our experimental facts, we believe that the transition from the case of single ions to clusters occurs at the concentration of $x = 0.05$ while the transition from the clusters to the array occurs between 0.1 and 0.2 of the relative concentration of Mn ions. The second threshold is less than the percolation threshold in the case of six nearest neighbours in the simple cubic lattice, which is 31% [20]; however, it corresponds well to the threshold for the percolation if we take into account 12 ions in the next coordination sphere.

There is no complete theory on combined exchange and JT dynamics of magnetic clusters in the literature yet, and we are suggesting only qualitative speculation. The ESR spectral behaviour of clusters is determined by two factors: the thermoactivated motion

(thermoactivated reorientations of the JT configurations), which explains the strong spectral narrowing with increase in temperature, and the exchange interaction between ions inside the cluster, which results in additional narrowing of the line. Obviously, the value of the activation energy estimated in our experiments corresponds to some average value because of the broad distribution in the cluster size and geometry.

Above the threshold of percolation, all or almost all Mn ions are linked by exchange interaction. The degree of the orbital ordering grows, and the effect of dynamic reorientations becomes non-significant. In this case, the spectral width is determined by the exchange and anisotropy [10, 11], whereas the dynamic JT narrowing occurs as a real phase transition at T_{JT} [12]. The evolution from finite clusters revealing the Arrhenius thermoactivated behaviour to the infinite array characterized by the co-operative phase transition has very general physical meaning and constitutes one of our main results.

Recently, Sanchez *et al* [21] studied the $LaGa_{1-x}Mn_xO_3$ crystals by means of x-ray absorption spectroscopy. They confirmed the instability of the Mn^{3+} octahedral local symmetry and claimed that most of the distortions are not due to the Jahn–Teller effect, either static or dynamic. It is interesting to note in this connection that only a minor part (about one tenth) of the Mn present in our samples (with $x = 0.05$ and 0.1) contributes to the temperature dependent EPR spectra shown in figures 1(b) and 4(a). Thus one can suppose that just this part of the Mn^{3+} ions constitutes clusters with symmetry properties allowing the JT configurations under discussion.

It is also appropriate to compare our EPR spectra (figures 1(b), 5, 6) with those reported for superparamagnetic systems (see, for example, [22, 23] and references therein). The superparamagnetic behaviour is commonly related to randomly distributed nano-size particles (clusters, droplets, etc), each of them being ordered ferromagnetically with a spontaneous magnetic moment $\mathbf{M}_i$ corresponding to 10^2–10^4 Bohr magnetons. At low temperatures, the overall ferromagnetic-resonance spectrum is strongly broadened due to random distribution in particle sizes, shapes, and orientations of the magnetic anisotropy axes. As the temperature increases, the magnetic (and anisotropy) energy of a particle becomes comparable with k_BT, and the thermal fluctuations of the $\mathbf{M}_i$ orientations lead to the narrowing of the spectrum. Such superparamagnetic behaviour looks very similar to that observed in our $LaGa_{1-x}Mn_xO_3$ samples with intermediate Mn concentrations ($x = 0.05$–0.1, figures 1(b), 4(a)). However, the existence of ferromagnetically ordered domains in these crystals can hardly be conceived in the temperature range of 120–300 K, where the thermally activated narrowing of the EPR line was observed (figure 4(a)). In fact, any ferromagnetic (or canted antiferromagnetic) state cannot be realized in the $LaGa_{1-x}Mn_xO_3$ system above 100–120 K; see the phase diagram at figure 12 in [6]. These arguments are more applicable to the oxygen deficient $LaMnO_{3-\delta}$ (figures 5, 6) where the thermally activated narrowing of the EPR line occurs at still higher temperatures (up to 500 K). Nevertheless, the similarity between our data and superparamagnetic ones has clear physical sense: in both cases, the narrowing of the magnetic-resonance spectra is caused by a thermally activated motion leading to partial averaging of the corresponding anisotropic part in the Hamiltonian. In superparamagnetic systems, such averaging is caused by thermal fluctuations of the $\mathbf{M}_i$ directions, whereas in the magnetically dilute manganites this is supposed to be due to the re-orientations of the JT distortions.

In conclusion, the effect of diamagnetic dilution on the ESR and spin dynamics was studied in the perovskite $LaGa_{1-x}Mn_xO_3$ single crystals. The evolution of the ESR spectrum was monitored from the many-component pattern characteristic of the single-ion picture up to the strong exchange narrowing at high Mn concentrations. In the intermediate region ($x = 0.05$–0.1), evidence was found for thermally activated internal motion which was attributed to re-orientations of the JT configurations over an energy barrier of about 50–100 meV. A

similar process was found to be characteristic for clusters of oxygen vacancies and Mn ions in $LaMnO_{3-\delta}$.

Acknowledgments

The authors thank G B Loutts, A R Kaul, O Yu Gorbenko, and A A Bosak for providing the samples under study, and D G Gotovtsev for technical assistance. The work was supported by NSF CREST project HRD-9805059, NASA project NCC3-1035, the Russian Foundation for Basic Research (grant No 02-02-16219), and the Programme for Basic Research 'Spin dependent effects in solids and spintronics' of the Russian Academy of Sciences.

References

[1] Coey J M D, Viret M and Von Molnar S 1999 *Adv. Phys.* **48** 167
[2] Dagotto E, Hotta J and Moreo A 2001 *Phys. Rep.* **344** 1
[3] Nagaev E L 2001 *Phys. Rep.* **346** 387
[4] Goodenough J B, Wold A, Arnott R J and Menyuk N 1961 *Phys. Rev.* **124** 373
[5] Zhou J-S, Yin H Q and Goodenough J B 2001 *Phys. Rev.* B **63** 184423
[6] Blasco J, Garcia J, Campo J, Sanchez M C and Subias G 2002 *Phys. Rev.* B **66** 174431
[7] Zhou J-S and Goodenough J B 2003 *Phys. Rev.* B **68** 144406
[8] Atsarkin V A, Demidov V V, Gotovtsev D G, Noginova N E, Bitok D and Bah R 2004 *Zh. Eksp. Teor. Fiz.* **126** 229 (in Russian)
Atsarkin V A, Demidov V V, Gotovtsev D G, Noginova N E, Bitok D and Bah R 2004 *JETP* **99** 202–10 (Engl. Transl.)
[9] Gudenko S V, Yakubovskii A Yu, Gorbenko O Yu and Kaul A R 2003 *Fiz. Tverd. Tela* **46** 2025 (in Russian)
Gudenko S V, Yakubovskii A Yu, Gorbenko O Yu and Kaul A R 2003 *Phys. Status Solidi* **46** 2094 (Engl. Transl.)
[10] Deisenhofer J, Eremin M V, Zakharov D V, Ivanshin V A, Eremina R M, Kruf von Nidda H-A, Mukhin A A, Balbashov A M and Loidl A 2002 *Phys. Rev.* B **65** 104440
[11] Huber D L, Alejandro G, Caneiro A, Causa M T, Prado F, Tovar M and Oseroff S B 1999 *Phys. Rev.* B **60** 12155
[12] Deisenhofer J, Kochelaev B I, Shilova E, Balbashov A M, Loidl A and Krug von Nidda H-A 2003 *Phys. Rev.* B **68** 214427
[13] Noginov M A *et al* 2000 *Magnetoresistive Oxides and Related Materials* (*MRS Symp. Proc.* vol 602) ed M S Rzchowski *et al* (Pittsburgh, PA: Materials Research Society) p 107
[14] Alejandro G, Passeggi M C G, Vega D, Ramos C A, Causa M T, Tovar M and Senis R 2003 *Phys. Rev.* B **68** 214429
[15] Slichter C P 1980 *Principles of Magnetic Resonance* (Berlin: Springer)
[16] Noginova N, Arthur E, Weaver T, Loutts G B, Atsarkin V A and Gotovtsev D G 2004 *Phys. Rev.* B **69** 124406
[17] Breen D P, Krupka D C and Williams F I B 1969 *Phys. Rev.* Ser. 2 **179** 241
[18] Noginova N, Loutts G B, Gillman E S, Atsarkin V A and Verevkin A A 2001 *Phys. Rev.* B **63** 174414
[19] Shengelaya A, Zhao G-M, Keller H, Müller K A and Kochelaev B I 2000 *Phys. Rev.* B **61** 5888
[20] Shklovskiy B I and Efros A L 1979 *Elektronnye svoystva legirovannyh poluprovodnikov (Electronic Properties of Doped Semiconductors)* (Moscow: Nauka) (in Russian)
[21] Sanchez M C, Subias G, Garsia J and Blasco J 2004 *Phys. Rev.* B **69** 184415
[22] Berger R, Bissey J-C, Kliava J, Daubric H and Estournes C 2001 *J. Magn. Magn. Mater.* **234** 535
[23] Kliava J and Berger R 2003 *Recent Res. Devel. Non-Cryst. Solids* **3** 41